Ocean Engineering 53 (2012) 138–152

Contents lists available at SciVerse ScienceDirect

Ocean Engineering

journal homepage: www.elsevier.com/locate/oceaneng

Cell-based evacuation simulation considering human behavior in a passenger ship

Sol Ha [a,1], Nam-Kug Ku [a,1], Myung-Il Roh [b,*], Kyu-Yeul Lee [a,c,2]

[a] Department of Naval Architecture and Ocean Engineering, Seoul National University, Daehak-dong, Gwanak-gu, Seoul 151-744, South Korea
[b] School of Naval Architecture and Ocean Engineering, University of Ulsan, Muger2-dong, Ulsan 680-749, South Korea
[c] Research Institute of Marine Systems Engineering, Seoul National University, Daehak-dong, Gwanak-gu, Seoul 151-744, South Korea

ARTICLE INFO

Article history:
Received 12 December 2011
Accepted 12 May 2012
Editor-in-chief: A.I. Incecik
Available online 25 July 2012

Keywords:
Evacuation simulation
Cell-based simulation
Human behavior
Passenger ship

ABSTRACT

Advanced evacuation analysis of passenger ships is a stochastic method in which the total evacuation time is calculated via computer-based simulations, by considering each passenger's characteristics (e.g., age, gender, etc.) and the detailed layout of the ship. This study presents simulations of advanced evacuation analysis using a cell-based simulation model for human behavior in a passenger ship. The cell-based simulation model divides the space in a uniform grid called *cell*. Each passenger is located in a cell and moves to another cell according to a set of local rules that are assumed to be associated with the individual, crowd, and counterflow-avoiding behaviors of the passengers. Individual behavior is described with the basic walking direction that a passenger will take during the evacuation. The change in the direction and speed of a passenger based on his/her interaction with the other passengers is expressed via the crowd behavior, which has three basic rules: separation, alignment, and cohesion. The passenger's behavior to avoid other passengers moving in the opposite direction is referred to as "counterflow-avoiding behavior" because such counterflow is included in the evacuation scenario. These behavior patterns are implemented as the local rules and are assigned to each cell. To verify the usefulness of the proposed simulation model, 11 tests specified in International Maritime Organization Maritime Safety Committee/Circulation 1238 (IMO/MSC Circ. 1238) were conducted, and it was confirmed that all the requirements of such tests had been met.

1. Introduction

In accordance with Circulation 1238 (Circ. 1238) of the International Maritime Organization (IMO) Maritime Safety Committee (MSC), entitled *Guidelines for Evacuation Analysis for New and Existing Passenger Ships*, a mandatory regulation issued by IMO, evacuation analysis should be performed for all passenger ships (IMO, 2007). The purpose of this regulation is to determine if the total evacuation time for a vessel is less than the allowable time according to the regulation. The maximum allowable time is 60 min for RORO (roll-on/roll-off) passenger ships and 80 min for regular passenger ships.

The guidelines offer the possibility of using two distinct methods for evacuation analysis: simplified evacuation analysis and advanced evacuation analysis. Simplified evacuation analysis is a deterministic method in which the total evacuation time is calculated using a simple hydraulic scheme, by considering that all passengers have identical characteristics. The total evacuation time can be calculated using a simple formula provided by the IMO, and the results should be submitted to the ship owner and the classification society. On the other hand, advanced evacuation analysis is a stochastic method in which the total evacuation time is estimated using a microscopic approach, by considering each characteristic of each passenger. In this analysis method, the total evacuation time is estimated via computer-based simulations that represent each passenger and the detailed layout of the vessel. Advanced evacuation analysis is currently not mandatory but is expected to be required in the future. Thus, a study on an advanced evacuation analysis was carried out in this paper.

The rest of this paper is as follows. Section 2 presents related studies on evacuation analysis and cell-based simulation techniques. Section 3 presents cell-based rules for human behavior in a passenger ship. Section 4 shows how to model passenger behavior based on the Cell–DEVS formalism, which is presented as a combination of discrete event system specifications (DEVS) and cellular automata. In Section 5, the results of 11 tests in IMO/MSC Circ.1238 and advanced evacuation analysis for a RORO passenger ship are explained to verify the passenger behavior model, and the aforementioned analysis method is compared

* Corresponding author. Tel.: +82 52 259 2165; fax: +82 52 259 2836.
E-mail addresses: miroh@ulsan.ac.kr (M.-I. Roh), kylee@snu.ac.kr (K.-Y. Lee).
[1] Tel.: +82 2 880 8378; fax: +82 2 886 4920.
[2] Tel.: +82 2 880 7327; fax: +82 2 888 9298.

0029-8018/$ - see front matter © 2012 Elsevier Ltd. All rights reserved.
http://dx.doi.org/10.1016/j.oceaneng.2012.05.019

with the commercial evacuation analysis program Evi. Finally, Section 6 presents the conclusions and future directions.

2. Related works

In recent years, researchers applied various approaches to study crowd evacuation under various situations, sometimes using such approaches separately or combining them. In Section 2.1, cellular automata models for evacuation analysis are reviewed. Sections 2.2 and 2.3 review the concepts of DEVS and Cell–DEVS, respectively.

2.1. Cellular automata models for evacuation analysis

Emergent evacuation is a system composed of many pedestrians characterized by strong interactions and environments. People want to move faster than usual in an emergent-evacuation scenario. The local interactions among pedestrians and those between pedestrians and the environment (e.g., a wall or a door) determine the global behavior of pedestrians. Various simulation models have been proposed to study the dynamics of evacuation. To simulate evacuation situations, it is important to comprehend the factors that affect passenger behavior, and to create a passenger behavior model that considers such factors.

Helbing and Molnar (1995) and Helbing et al. (2000) proposed a social-force model for pedestrians' continuous motion. In this model, pedestrians are treated as particles subject to long-range forces induced by the social behavior of individuals. The movement of pedestrians can be described with a main function, which determines the physical and social forces, and the induced velocity changes. The social-force model is determined by the acceleration equation. In recent years, social-force models were further developed to study crowd evacuation (Zheng et al., 2002; Seyfried et al., 2006). Referring to these social forces, Cho et al. (2010) and Cho (2011) modeled passenger behavior as velocity-based, taking into account different aspects of human behavior in an evacuation. They suggested that passenger behavior consists of individual, crowd, and counterflow-avoiding behaviors. Using this model, they developed an advanced evacuation analysis program for passenger ships. This program was verified with the 11 tests specified in IMO/MSC Circ.1238 and was applied to a RORO passenger ship.

Cellular automata models have also been developed to study crowd evacuation under various situations. A cellular automata model quantifies the evacuation area in terms of discrete cells. Each cell can be empty or occupied by a pedestrian or an obstacle object. A pedestrian can move to an empty neighboring cell in each time step.

Cellular automata models can be classified into two categories. The first category is based on the interactions between environments and pedestrians. For example, Zhao et al. (2006) proposed a two-dimensional cellular automata random model to study the exit dynamics of an occupant evacuation. Song et al. (2006) and Yu and Song (2007) proposed a cellular automata model without a step back to simulate the pedestrian counterflow in a channel considering the surrounding environment. These models demonstrate that various environments, such as the exit width and obstacles, have an impact on the pedestrian movement. The second category is based on the interaction among pedestrians. Kirchner et al. (2003) proposed a cellular automata model for pedestrian dynamics with friction to simulate competitive egress behavior. Kirchner and Schadschneider (2002) proposed a bionics-inspired cellular automata model to describe the interaction among the pedestrians and to simulate evacuation from a large room with one or two doors. Additionally, Weng et al. (2006) proposed a cellular automata model without a swith different walking velocities.

As mentioned above, the observed phenomena that occur during evacuations have been reproduced by these models in the last few years. Due to the complex rules of the social-force model, it does not offer good calculation efficiency. On the other hand, cellular automata models are discrete in space, time, and state variables. This makes the models ideally suited for large-scale computer simulation. As the advanced evacuation analysis for passenger ships is intended for thousands of passengers, the cellular automata model was adopted in terms of its performance. Therefore, the three passenger behaviors proposed by Cho et al. (2010) and Cho (2011) were modeled as cellular automata in this study.

2.2. DEVS (discrete event system specifications) formalism

Praehofer and Zeigler proposed a modeling and simulation method that can handle simulation models of a discrete event and a discrete time (Praehofer, 1992; Zeigler et al., 2000). This method, called discrete event system specifications (DEVS) and discrete time system specifications (DTSS) formalism, is widely used as a standard for modeling and simulation.

DEVS formalism consists of two models: the atomic model and the coupled model. The atomic model shown in Fig. 1 is the basic model and has specifications for the dynamics of the model. The coupled model, on the other hand, provides the method of assembly for several atomic and/or coupled models to build a complex system hierarchy.

Bang and Cha developed a simulation framework based on the combined DEVS/DTSS concepts (Bang, 2006; Cha et al., 2009; Ha et al., 2009; Cha et al., 2010). To evaluate the efficiency and applicability of the simulation framework, Bang and Cha applied it to the block erection process in shipbuilding and underwater warfare simulation.

2.3. Cell–DEVS

In the studies of Wainer and Giambiasi (2002) and Wainer (2009), the Cell–DEVS formalism was presented as a combination of DEVS and cellular automata with explicit timing delays, which are discrete time steps for updating the state of each cell. DEVS formalism is one of the discrete-event modeling and simulation techniques that were based on systems theory concepts. Cell–DEVS formalism describes cell spaces as discrete event models, wherein each cell is seen as a DEVS atomic model that can be updated at each time step. This approach is still based on the formal specifications of DEVS, but it allows the user to focus on the problem to be solved using simple rules for modeling, as with CA. Wainer (2009) applied Cell–DEVS formalism to various fields, including biology, emergency planning, and chemistry. Ha et al. (2011) simulated the oil slick movement based on Cell–DEVS formalism.

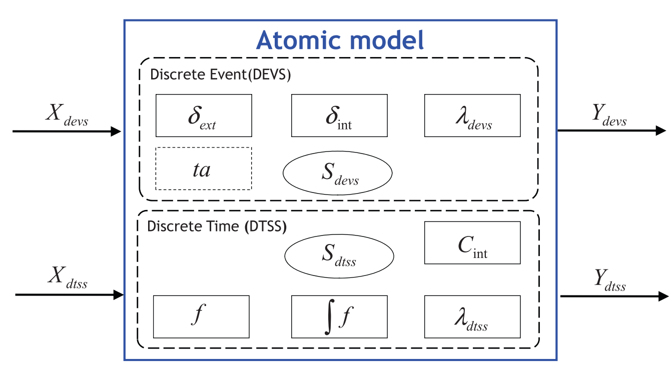

Fig. 1. Configuration of the combined DEVS/DTSS atomic model.

This approach allows the enhancement of different aspects of the modeling experience. The formal definition of cell spaces simplifies the construction of new models. Cell–DEVS formalism is more efficient than cellular automata in terms of performance because only active cells execute their local computing function. For this reason, the passenger behavior model was implemented based on Cell–DEVS.

3. Modeling of Human behavior in a passenger ship

As mentioned in Section 2.1, the passenger behavior proposed by Cho et al. (2010) and Cho (2011) modeled passenger behavior based on velocity. To improve performance of evacuation analysis, this model was converted into a cellular automata model based on Cell–DEVS. In this section, the cellular automata modeling of the passenger behavior is described in detail.

3.1. Overview

This section focuses on passenger behavior, specifically state transition of the passenger flow during an evacuation, and the relationship between the passengers. The two-dimensional cellular automata model and the continuous passenger behavior proposed by Cho et al. and Cho, respectively, were used.

Generally, the passengers try to move quickly towards the exits, avoid colliding with one another, and sometimes go with the crowd during an evacuation. These can be characterized by discrete individual, crowd, and counterflow-avoiding behaviors, which indicate various interactions, including position attraction, separation caused by the surrounding passengers, and movement direction.

A network of cells was applied in this study. Each cell was 0.4×0.4 m big, which is the typical space occupied by a passenger in a dense crowd. Therefore, each cell could be either empty or occupied by only one passenger. The cell was allowed to be in only one of the following three main states at any time: empty, occupied, and obstacle.

Individuals may have various walking speeds according to their age and gender. IMO/MSC Circ. 1238 recommended walking speeds based on ages and genders. In this study, 0.8 m/s was adopted as the average walking speed, which is a typical value in a dense crowd. Thus, one time step in the model corresponds to 0.5 s, according to the size of each cell. The change in the walking speed with the crowd density during an evacuation was not considered.

In a von Neumann neighborhood (Von Neumann, 1966), four directions are taken into account (up, down, left, and right), whereas in a Moore neighborhood, eight directions, including diagonal directions, are considered. Although the von Neumann neighborhood is simpler, it is not as accurate as the Moore neighborhood.

In this study, the Moore neighborhood was adopted to determine the movement direction of the occupants because eight directions can more accurately describe the movement of evacuees.

The passenger behavior rules for evacuation deal with movement to the destination, interaction between passengers, and interaction between passengers in different directions. These rules are detailed in Sections 3.2, 3.3, and 3.4.

3.2. Individual behavior

Cho (2011) modeled individual behavior by sequentially defining the walking speed and the walking direction. He determined the walking direction by identifying the shortest-distance route to a destination using a visibility graph. When the escape route is determined, the walking direction can be found along the escape route. A combination of the visibility graph and the Dijkstra algorithm was used to calculate the shortest-distance route to a destination, considering the obstacle in the compartment. This study calculates the shortest distance to the destination using these combined algorithms.

The steps in calculating the shortest distance using a visibility graph are summarized as follows (Fig. 2):

(1) Create the vertices at the center of the door, at the corners of the obstacles, and at the center of the passengers [see Fig. 2(a)].
(2) Bond the vertices with lines that are visible to one another, and make a graph [see Fig. 2(b)].
(3) Determine the shortest-distance route in the graph using the Dijkstra algorithm [see Fig. 2(c)], and calculate the shortest distance to the final destination [see Fig. 2(d)].

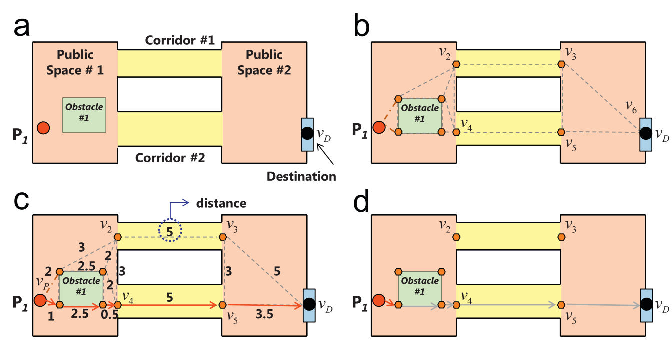

Fig. 2. Steps in calculating the shortest distance: (a) create the vertices of the graph; (b) bond the vertices with lines that are visible to one another; (c) determine the shortest-distance route in the graph; and (d) calculate the shortest distance.

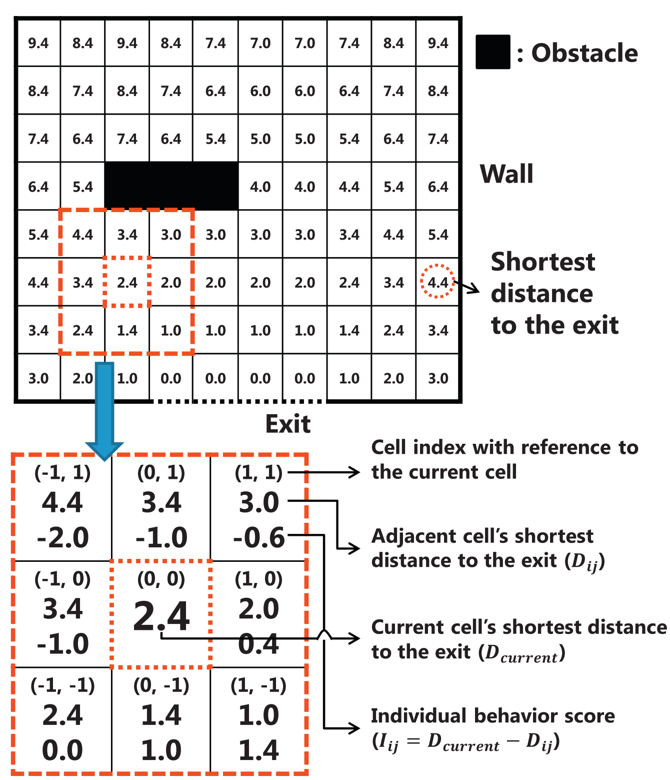

Fig. 3. Shortest-distance grid for the simple compartment.

As mentioned above, calculating the shortest distance considering the visibility of the passenger means determining the shortest direction by creating a new visibility graph for each time unit. As this is a very expensive and time-consuming procedure for thousands of passengers, however, the compartments were discretized into cells, and the representative shortest distance for each cell was determined and stored in cells in advance to start an evacuation analysis, as shown in Fig. 3.

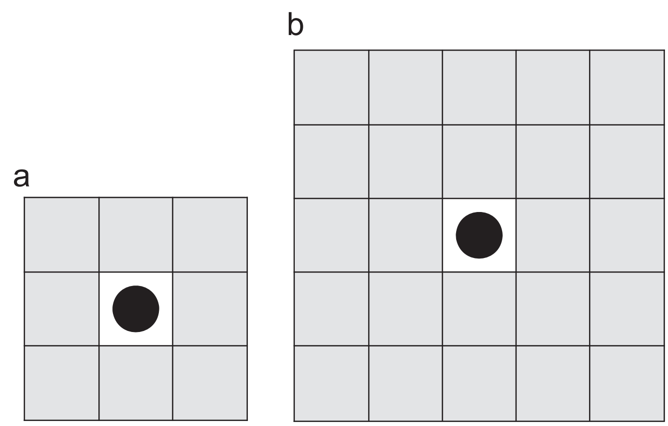

Fig. 4. Interaction radius (R_i) for the crowd and counterflow-avoiding behaviors. (a) R_i=1 and R_i=2.

The cell index with reference to the current cell is shown in Fig. 3. The cell index is defined as a vector (i, j), wherein the first component i is increased by 1 for each step from left to right, and j, for each step from down to up.

After the calculation of the shortest distance of each cell, the score for the individual behavior I_{ij} was calculated using Eq. (1). The individual behavior score did not evolve with time and did not change with the presence of passengers.

$$I_{ij} = D_{current} - D_{ij}. \tag{1}$$

In the equation above, $D_{current}$ is the shortest distance from the current cell to the exit, and D_{ij} is the shortest distance from the neighbor cell (i,j) of $D_{current}$ to the exit.

3.3. Crowd behavior

This section describes the crowd behavior that causes the interaction among the passengers. Before describing the crowd and counterflow-avoiding behaviors, the interaction radius (R_i) is introduced. Particles make judgments after collecting information on an area within the R_i cells around the current position of the passenger. Take $R_i = 1$ as an example in Fig. 4(a). The particles will look at the $8[=(R_i x2+1)^2-1]$ cells (i.e., at all the cells around), except for the central one, before the passenger decides which way to move. In this paper, the interaction radius was set at 3.

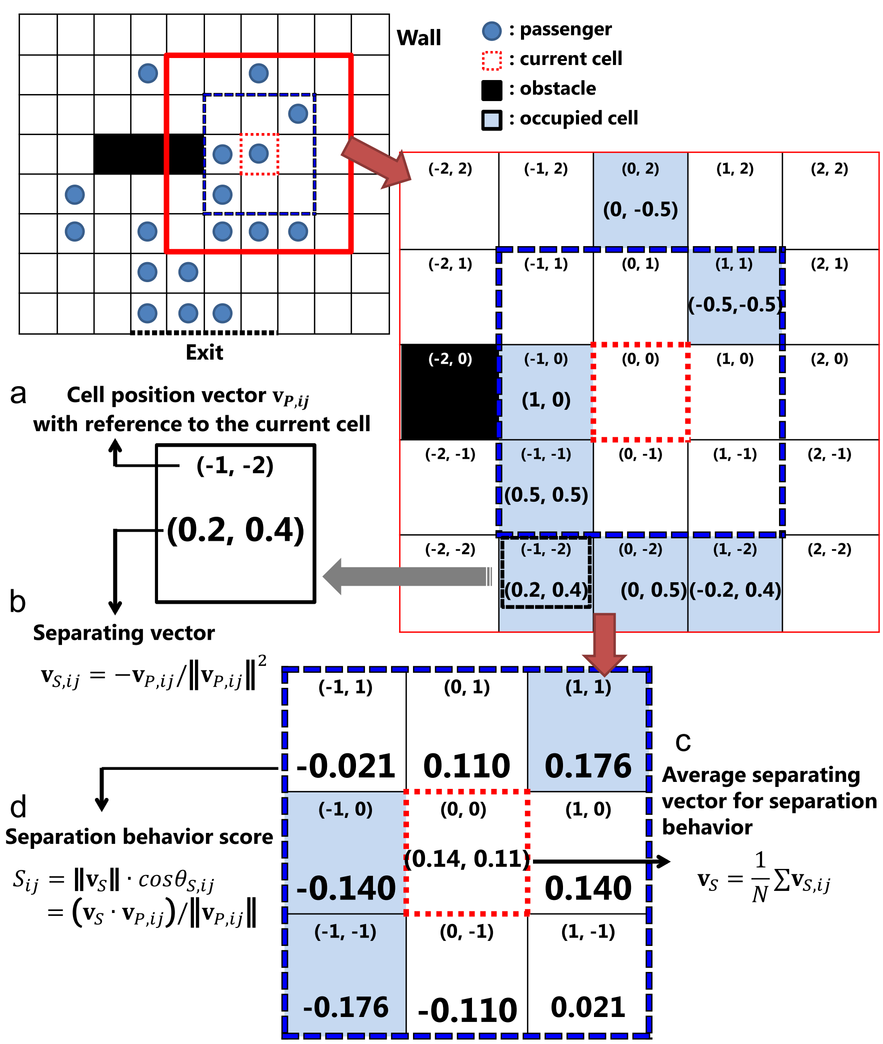

Fig. 5. Example of the calculation of the separation behavior score of the neighbor cells.

During an evacuation, passengers tend to act together with other passengers. For example, passengers want to use the same exit used by other passengers, even though there are other exits. The flock algorithm suggested by Reynolds (1987, 1999) and Hartman and Benes (2006) is used for modeling passengers' flock behavior. Flock behavior is a result of the motion and interaction of passengers. Each passenger has three local rules of behavior: separation, cohesion, and alignment.

3.3.1. *Separation behavior*

Each passenger in a crowd tends to avoid collision with his neighbors. This tendency is called *separation or collision avoidance*, which signifies efforts to avoid overcrowding local neighbors. The separation vector is simply calculated with the index of each cell occupied by a passenger.

As shown in Fig. 5, the interaction range R_i was set at 2. The current cell (0, 0) has 24 adjacent cells because the interaction range R_i is 2 and has seven occupied cells in Fig. 5. Each cell's position vector $\mathbf{v}_{P,ij}$ with reference to the current cell is the same as the cell index [see Fig. 5(a)].

The separating vector $\mathbf{v}_{S,ij}$ of the occupied cell in the interaction range $R_i$can be calculated as in the following equation [see Fig. 5(b)]:

$$\mathbf{v}_{S,ij} = -\frac{\mathbf{v}_{P,ij}}{\|\mathbf{v}_{P,ij}\|} \cdot \frac{1}{\|\mathbf{v}_{P,ij}\|}. \tag{2}$$

As an example of cell (1,–2), its unit position vector$\mathbf{v}_{P,ij}/\|\mathbf{v}_{P,ij}\|$ is $(1/\sqrt{5},-2/\sqrt{5})$, and the length of position vector $\mathbf{v}_{P,ij}$ is $\sqrt{5}$. Therefore, the separating vector of cell $(-1,-2)$ can be calculated as $(-1/5,2/5)=(-0.2,0.4)$ using Eq. (2). Similarly, the separating vectors of the seven occupied cells can be calculated.

Using these separating vectors, the separation behavior score can be determined using the following equations [see Fig. 5(c) and (d)]:

$$\mathbf{v}_S = \frac{1}{N}\sum \mathbf{v}_{S,ij}, \tag{3}$$

and

$$S_{ij} = \|\mathbf{v}_S\| \cdot \cos\theta_{S,ij} = (\mathbf{v}_S \cdot \mathbf{v}_{P,ij})/\|\mathbf{v}_{P,ij}\|. \tag{4}$$

Here, $\mathbf{v}_S$ is the average of the separating vectors in the occupied adjacent cells, N is the number of occupied neighbor cells (N=7 in Fig. 5), and $\theta_{S,ij}$ is the angle between the average separating vector $\mathbf{v}_S$ and each cell's position vector $\mathbf{v}_{P,ij}$.

As shown in Fig. 5, the average separating vector $\mathbf{v}_S$ is (0.14, 0.11), which is the average of the separating vectors in the seven occupied cells among 24 adjacent cells. Using Eq. (4), the separation behavior score of cell $(1,\ -1)$ is calculated as 0.021. The separation behavior score is calculated for eight neighbors of the current cell (0, 0).

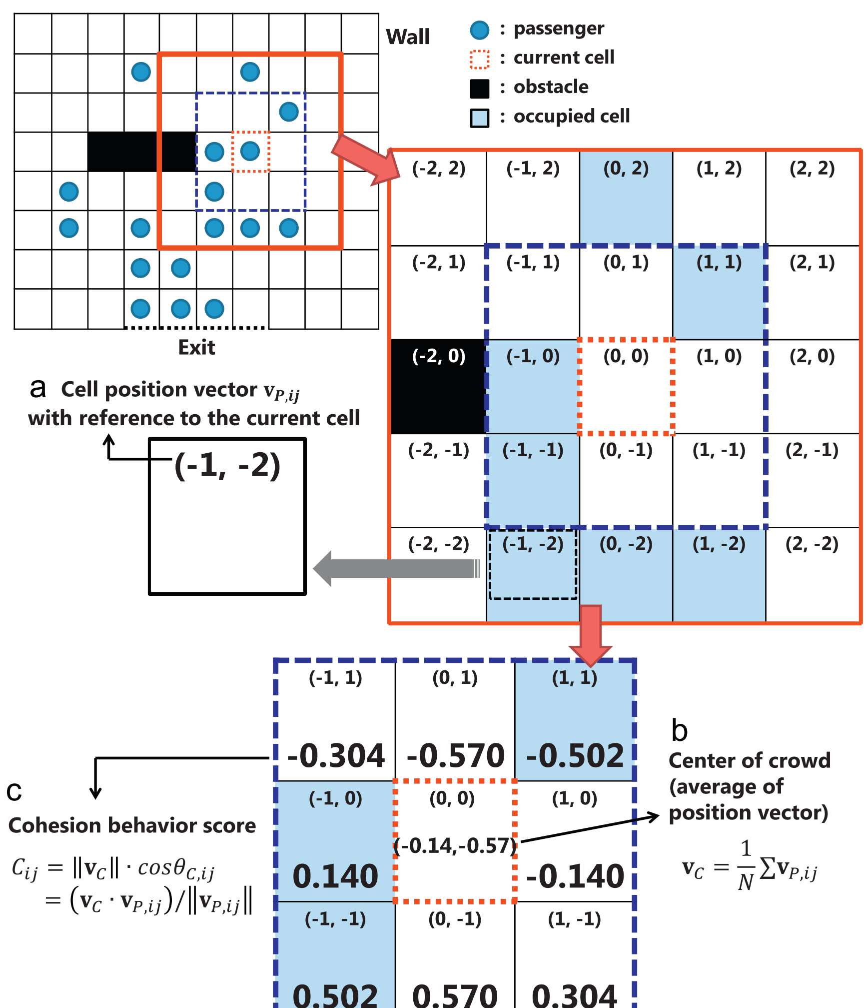

Fig. 6. Sample calculation of the cohesion behavior score of the neighbor cells.

3.3.2. Cohesion behavior

Passengers tend to stay close to the center of the local group formed by neighbors, and to find comfort within the group. This tendency is called *cohesion*.

As shown in Fig. 6, interaction range R_i and each cell's position vector $\mathbf{v}_{P,ij}$ are the same as the example in Section 3.3(a). The cohesion behavior score can be determined using the following equations:

$$\mathbf{v}_C = \frac{1}{N}\sum \mathbf{v}_{P,ij}, \tag{5}$$

and

$$C_{ij} = \|\mathbf{v}_C\| \cdot \cos\theta_{C,ij} = (\mathbf{v}_C \cdot \mathbf{v}_{P,ij})/\|\mathbf{v}_{P,ij}\|. \tag{6}$$

Here, $\mathbf{v}_C$ is the center of the crowd in interaction range R_i, which is the average position vector of the occupied cell; and $\theta_{C,ij}$ is the angle between $\mathbf{v}_C$ and each cell's position vector $\mathbf{v}_{P,ij}$.

As shown in Fig. 6, the center of crowd $\mathbf{v}_C$ was $(0,-2)$, which was the average position vector of the seven occupied cells among the 24 adjacent cells. Using Eq. (6), the cohesion behavior score of neighbor cell $(1,\ -1)$ was determined to be 0.304. The cohesion behavior score was calculated for the eight neighbors of the current cell (0, 0).

3.3.3. Alignment behavior

Passengers tend to match the direction and speed of their neighbors. This is the factor that causes passengers to follow one another. It is called *alignment behavior*.

As shown in Fig. 7, interaction range R_i and each cell's position vector $\mathbf{v}_{P,ij}$ are the same as the example in Section 3.3(a). The passenger occupying each cell had the previous direction vector $\mathbf{v}_{A,ij}$, which refers to his/her direction in the previous time step. As an example of cell $(1,-2)$, the passenger in this cell was moved from cell $(0,-3)$. From this, it can be known that the moving direction in the previous time step was $(1/\sqrt{2},1/\sqrt{2})$, and that this was the previous direction vector $\mathbf{v}_{P,ij}$ of cell (1,–2). The alignment behavior score can be determined using the following equation:

$$\mathbf{v}_A = \frac{1}{N}\sum \mathbf{v}_{A,ij}, \tag{7}$$

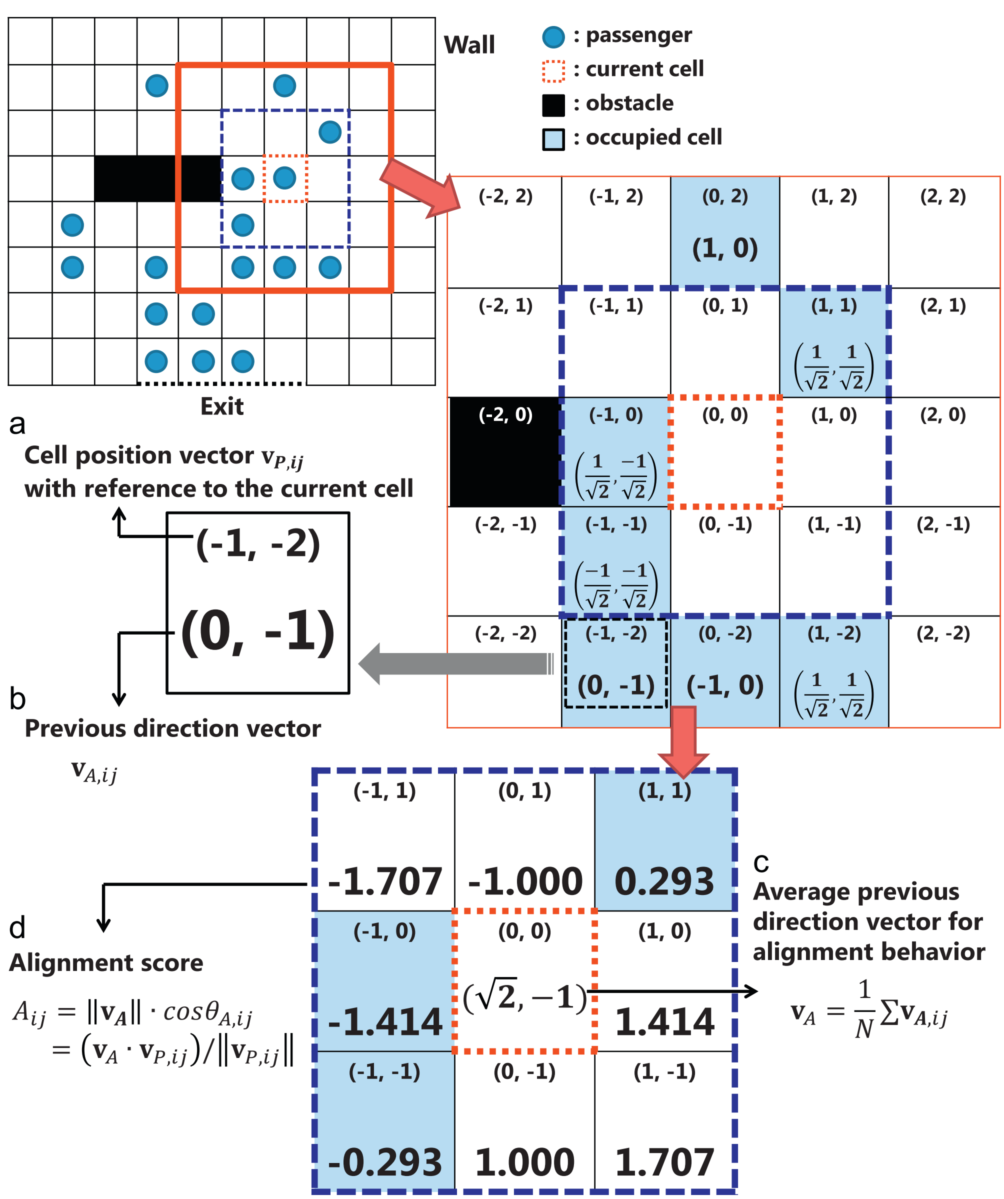

Fig. 7. Sample calculation of the score for the alignment behavior.

and

$$A_{ij} = \|\mathbf{v}_A\| \cdot \cos\theta_{A,ij} = (\mathbf{v}_A \cdot \mathbf{v}_{P,ij}) / \|\mathbf{v}_{P,ij}\|. \tag{8}$$

Here, $\mathbf{v}_A$ is the average of the previous direction vectors $\mathbf{v}_{A,ij}$ in the occupied cells among the adjacent cells, and $\theta_{A,ij}$ is the angle between vector $\mathbf{v}_A$ and each cell's position vector $\mathbf{v}_{P,ij}$.

In Fig. 7, the average of the previous direction vector $\mathbf{v}_A$ was determined to be $(\sqrt{2}, -1)$. Using Eq. (8), the alignment behavior score of the neighbor cell $(1, -1)$ was determined to be 1.707. The alignment behavior score was calculated for the eight neighbors of the current cell (0, 0).

After the calculation of the scores for the separation, cohesion, and alignment behaviors, the score for crowd behavior C_{ij} was determined from the combination of these scores, using Eq. (11), where K_S, K_C, and K_A are the weighting factors of each behavior.

$$C_{ij} = K_S \cdot S_{ij} + K_C \cdot C_{ij} + K_A \cdot A_{ij}. \tag{9}$$

To determine these weighting factors of each behavior, several simulations were performed, and the results were compared with the passenger behavior in the previous study (Cho, 2011). By comparing the results and modifying the weighting factors, the following weighting factors were determined: $K_S = 1.0$; $K_C = 0.2$; and $K_A = 0.3$.

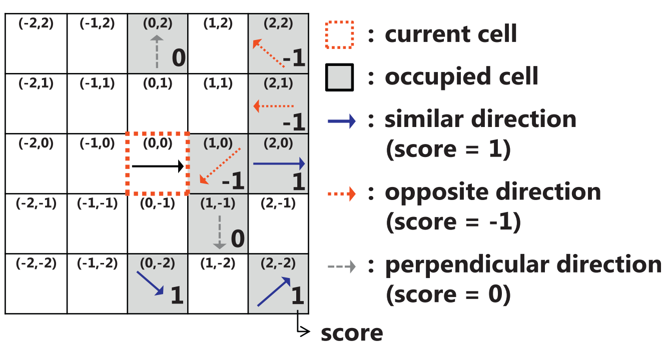

Fig. 8. Sample scoring of the occupied cell before the calculation of the counter-flow-avoiding behavior.

3.4. Counterflow-avoiding behavior

As mentioned in Section 3.3(a), if the separation behavior will be considered, passengers can keep their distance from one another. If the passengers, however, are located in an area with a high population density, and if the separation behavior is considered without distinguishing if the neighbor is walking in the same direction or in the opposite direction, the passengers can be congested and stuck in a crowd. Therefore, they need to change their walking direction to directions aimed at avoiding the passengers walking in the opposite direction as well as for following the passengers walking in the same direction. This is called *counterflow-avoiding behavior* and is modeled in reference to the study of Cho (2011).

The objective of counterflow-avoiding behavior is to modify the direction with the largest forward flow. In this case, the counterflow is considered a negative forward flow, and the passengers also tend to avoid directions with counterflow. At each time, passengers have three options: to keep going forward, to change their walking direction to the right, or to change their walking direction to the left.

The counterflow-avoiding behavior follows a certain sequence. The basic idea of such behavior is to choose the sector with the least counterflow. As shown in Fig. 8, interaction range R_i was 2, and a passenger in the current cell (0, 0) headed for the right side. Each occupied cell can be scored using the following rule:

$$T_{ij} = \begin{cases} 1 & \text{similar direction,} \\ 0 & \text{perpendicular direction,} \\ -1 & \text{opposite direction.} \end{cases} \tag{10}$$

For example, as cell (2, 0) headed for the right side, which was the same as the direction of the current cell, it was scored 1. Similarly, as cell (1, 0) headed for the left-bottom side, it was scored -1.

Thereafter, the area in front of the passenger was divided into three overlapping sectors, as shown in Fig. 9. The dividing area was fan-shaped in the study of Cho (2011) but was divided into rectangles because all the spaces were divided into discrete cells. To make sure that all the sectors have the same area, interaction radius R_i should have an even value.

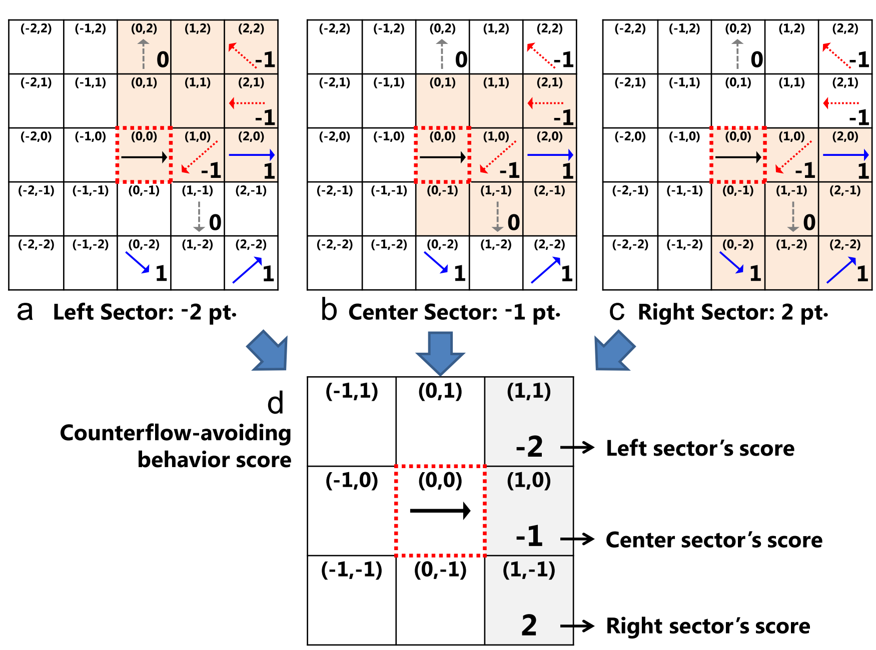

Fig. 9. Division of the area in front of the passenger into three overlapping sectors, and scoring of each sector.

After the division of the sectors, the scores of the occupied cells in each sector were summarized. For example, the score of the left sector in Fig. 9(a) was -2, and the score of the right sector in Fig. 9(c) was 2. Then the sector with the highest score was chosen. As the selected sector had more passengers with similar directions, it can be thought that the direction towards the selected sector is more suitable than the other direction. In Fig. 9, as the right sector has the highest score, the direction towards that of cell $(1, -1)$ should be chosen. The counterflow-avoiding behavior score was calculated only for three neighbor cells in front of the passenger direction.

$$CF_{ij} = \sum (T_{ij} \text{ of each sector}) \tag{11}$$

3.5. Cellular automata model of passenger behavior

Based on the passenger behaviors described in Sections 3.2, 3.3, and 3.4, the evacuation process of passengers is realized as follows:

Rule 1. Update the individual behavior score
Read the compartment information on the passenger ship and calculate the individual behavior score of each grid in advance to start the evacuation. This rule is executed only once.
FOR EACH (every cell):
Update the distance to the exit.
Update the individual behavior score.

Before starting the evacuation, the representative shortest distance from each cell to the exit is determined and stored in each cell in advance. As mentioned in Section 3.2, the individual behavior score is also calculated using these distances.

Rule 2. Update the crowd and the counterflow-avoiding behavior score
Determine the scores of the crowd and counterflow-avoiding behaviors for each occupied cell.
FOR EACH (every occupied cell):
Update the **crowd behavior score.**
Update the **counterflow-avoiding behavior score.**

The crowd and counterflow-avoiding behavior scores are updated at each time step using the equations shown in Sections 3.3 and 3.4, respectively.

Rule 3.Update the total score and the moving direction
Together with the scores found in rules 1 and 2, calculate the total score of each adjacent grid for each occupied cell, and judge everyone's moving direction in the next time step.
FOR EACH (every occupied cell):
Update the total score.
Update the moving direction.

Fig. 10 shows an example of the updation of the rule in the cellular automata model for passenger evacuation. As shown in Fig. 10, each cell has only one state among the following three states: empty, occupied, and obstacle. To move each passenger to the neighbor cell, the total score of the eight neighbor cells for each occupied cell should first be calculated.

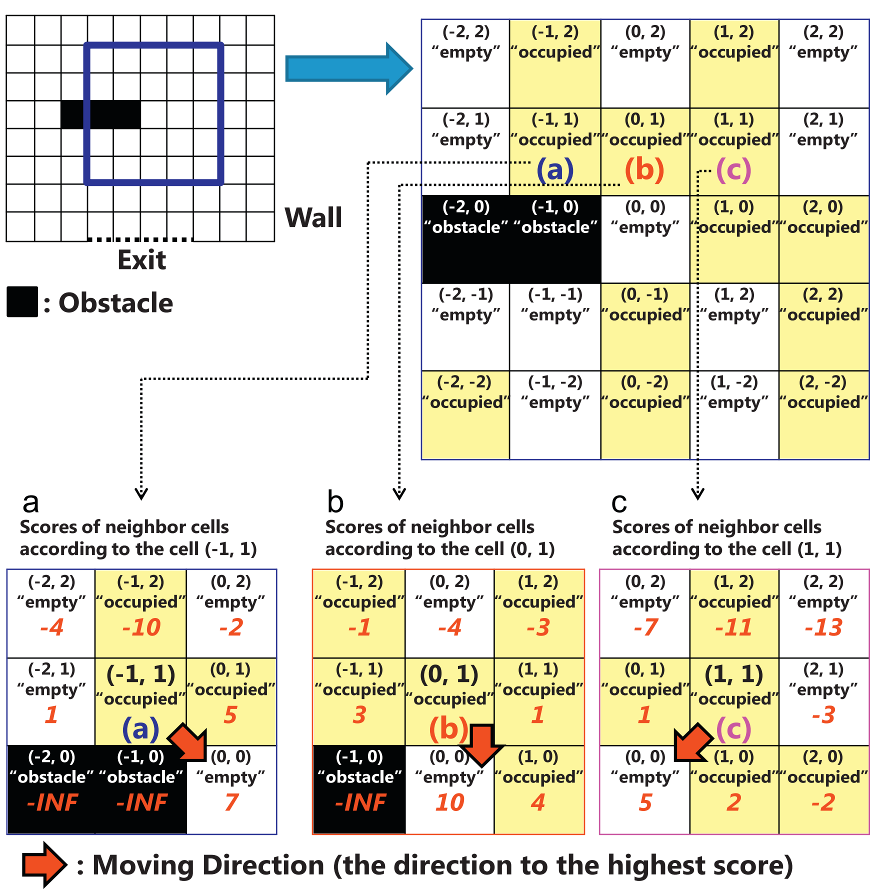

Fig. 10. Updating the neighbor cell's score for all the occupied cells, and choosing the moving direction.

The total score, which determines where the evacuee will move in the next time step, is a superposition of the individual, crowd, and counterflow-avoiding behavior scores. Among all the possible target grids, the grid that has the highest score will be chosen as the next position in the next time step. This process is shown in the following equation:

$$G_{ij} = [(I_{ij} \times K_I) + (C_{ij} \times K_C) + (CF_{ij} \times K_{CF})]\xi_{ij}, \tag{12}$$

with the following obstacle number:

$$\xi_{ij} = \begin{cases} -\infty & \text{for forbidden cells (wall, obstacle)}, \\ 1 & \text{otherwise}. \end{cases} \tag{13}$$

G_{ij} is the score that is used when the passenger chooses neighbor grid (i,j) as the next destination. I_{ij} is the score for the individual behavior, which represents the factors related to the position of the grid and the distance to the destination, and is associated with the behavior of each passenger. C_{ij} is the score for the crowd behavior between passengers. CF_{ij} is the score for the counterflow-avoiding behavior between the passengers in the other groups. K_I, K_C, and K_{CF} are the weighting factors of the individual, crowd, and counterflow-avoiding behaviors. These weighting factors were also determined by comparing them with the corresponding values obtained in the previous study (Cho, 2011). In this study, the weighting factors K_I, K_C, and K_{CF} were set at 1.0, 0.8, and 1.1, respectively. For example, the total score of the eight neighbor cells of the occupied cells $(-1, 1)$, $(0, 1)$, and $(1, 1)$ in Fig. 10 can be calculated using Eq. (12).

Assume that the scores of the eight neighbor cells have already been calculated, as shown in Fig. 10(a), (b), and (c). In the case of the occupied cell $(-1, 1)$, its neighbor cell $(0, 1)$ will have a score of 5, and its neighbor cell $(0, 0)$ will have a score of 7. Thus, the moving direction of the occupied cell $(-1, 1)$ will be the right-bottom direction of the cell, as shown in Fig. 10(a). Similarly, the moving direction of cell $(0, 1)$ will be the bottom direction, and the moving direction of cell $(1, 1)$ will be the left-bottom direction of the cell.

Rule 4. Move and conflict

If a conflict occurs, as several passengers have chosen the same grid, only the one with the highest score can be kept going to the selected cell, and all the others should be returned to their original positions.

FOR EACH and every occupied cell:

Move the passenger to the neighbor cell in the moving direction.

IF (in the case of passenger conflict):

Select only one passenger—the one who has the highest score.

Move the selected passenger.

Return all the other passengers to their original positions.

As mentioned in the previous paragraph, as cells $(-1, 1)$, $(0, 1)$, and $(1, 1)$ chose the moving direction towards cell $(0, 0)$, the three

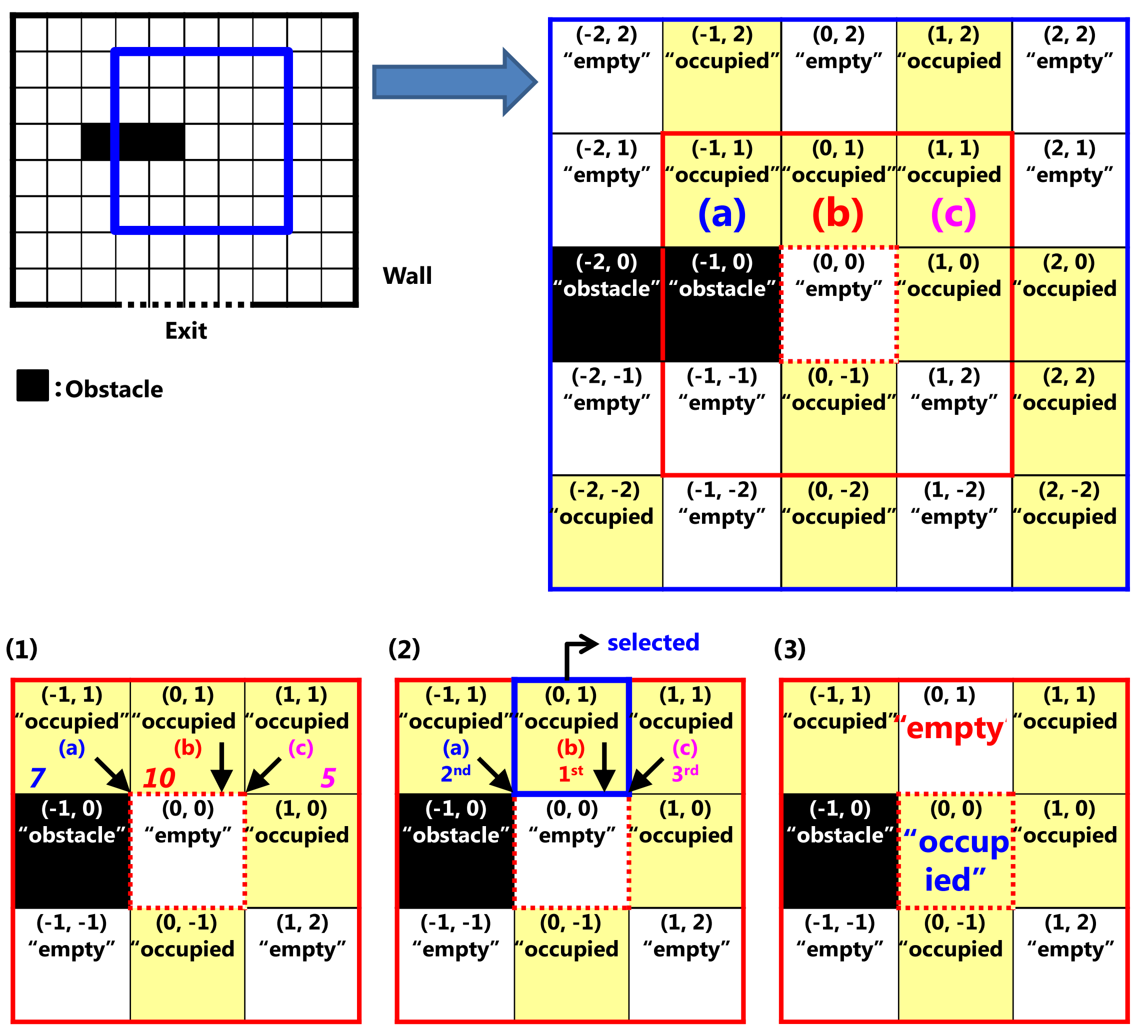

Fig. 11. Updating the rule to move a passenger to an empty neighbor cell.

passengers may conflict with one another. If a conflict occurs, the passenger who has the highest score can be kept going towards the moving direction, and the others can stay in their original positions. In Fig. 11(1), the score of cell $(-1, 1)$ to the direction of cell (0, 0) is 7, the score of cell (0, 1) is 10, and the score of cell (1, 1) is 5. Therefore, cell (0, 1) has the highest score, and is chosen. As shown in Fig. 11(3), as the passenger in cell (0, 1) moved to cell (0, 0), the state of cell (0, 1) was changed to empty, and the state of cell (0, 0) was changed to be occupied. Additionally, it can be seen that the passengers in the other cells kept their positions.

Rule 5. End or Repeat
After the updation of the position of each passenger, the time goes on with a discrete time step. Check the position of each passenger. If all the passengers are in their respective destinations, the evacuation is ended. If not, rule 2 is run again.
IF (update is completed):
The time interval progresses.
IF (all the passengers are in their respective destinations):
End of evacuation
ELSE
Run ***rule 2*** again.

If the position of each passenger is fully updated, the simulation time goes on with a discrete time step. After this, it is checked if all the passengers are already in their respective destinations. If they are, the evacuation process is ended. If not, rules 2, 3, 4, and 5 are repeated.

4. Implementation of the passenger behavior model based on Cell–DEVS

To conduct advanced evacuation analysis, the compartments of the ship were first modeled. Fig. 12 shows the results of the modeling of the passenger ship's compartments based on the cells.

Each cell adopted the atomic model using the Cell–DEVS formalism. As shown in Fig. 12, the atomic model of each cell has seven basic components: the state variable, input port, output port, external transition function, internal transition function, output function, and time advance function. Using the pseudo code, each component of the atomic model is described in detail below.

4.1. State variables

The state variables in each cell are defined as follows:

$S_{devs} = \{Phase, Update, Info, Person, Neighbors\}.$

As mentioned earlier, the cell has three basic states: empty, occupied, and obstacle. Three dummy states were added: the leaving and occupying states for sending the output to the adjacent cells, and the "returning" state to return the conflicted passenger. These states are stored in the state variable *Phase*. The cell has an additional state variable. *Update* represents information on whether or not the cell was updated at the current time; *Info*, information on the current cell; *Person*, information on the passenger occupying the current cell; and *Neighbors*, information on the adjacent cells.

4.2. Input and output ports

The model has two input ports: *inCellInfo* and *inPerson*. The inCellInfo input port allows the cell to receive information from the neighbor cell. The *inPerson* input port allows the cell to receive information on the occupying passenger. The cell model also has two output ports: *outCellInfo* and *outPerson*. The *out-CellInfo* output port outputs the cell information to the adjacent cells. The *outPerson* output port of the current cell is dynamically connected to the *inPerson* input port of the neighbor cell when the passenger in the current cell moves to the neighbor cell.

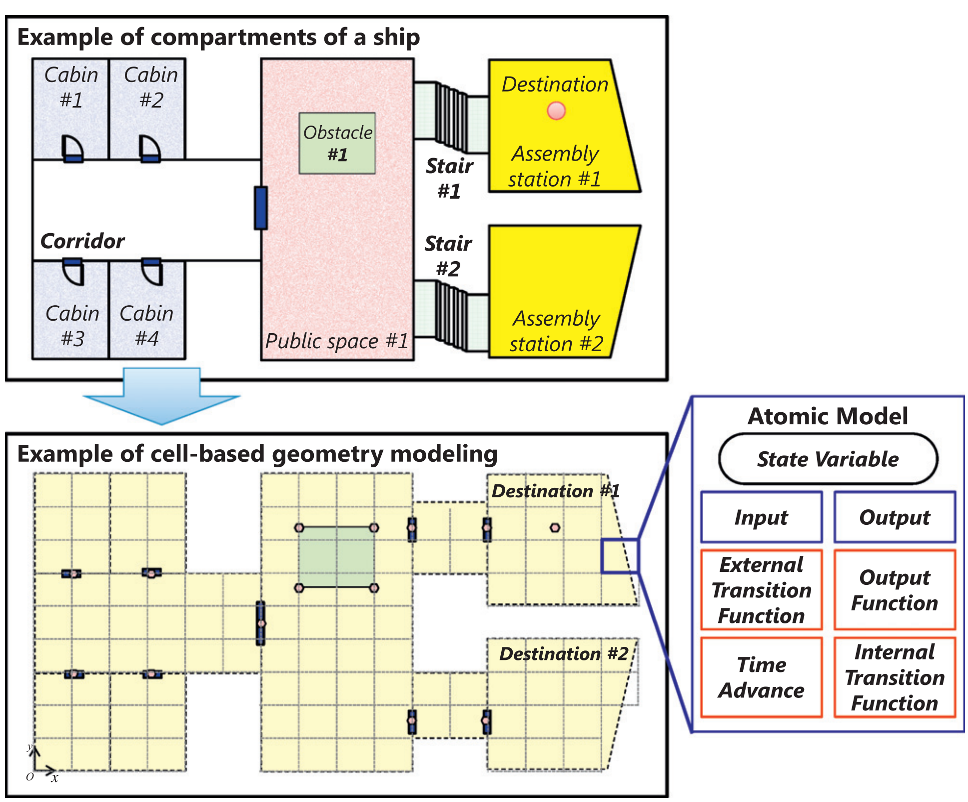

Fig. 12. Cell-based modeling of the compartments of a passenger ship.

4.3. External transition function

If there is an *inPerson* input, the phase of the cell is changed to the occupying state, and the cell stores the data of the passenger to the person state variable. If a conflict occurs, only the cell with the highest score can be chosen, and the state of the cell is changed to the returning state. When the passenger returns, the state of the cell is changed to the occupied state. If there is an input from the neighbor cell, the cell stores the information transmitted by the neighbor cell.

```
IF (Update=Updating)
  IF (there is an inPerson input)
    IF (Phase=Empty)
      Phase=Occupying, Person=inPerson
    ELSEIF (Phase=Occupying or occupied)
      IsReturn=SelectPassenger (Person, in Person)
    IF (IsReturn=true)
      Phase=Returning
    ELSE IF (Phase=Leaving and in Person=Person)
      Phase=Occupied
IF (there is an inCellInfo input)
  Neighbors=UpdateNeighbors (inCellInfo)
OTHERWISE
  Nothing; wait for the elapsed time
```

4.4. Output function

If the cell is in the ready state, it transmits information on the current cell to the neighbor cells. If the cell is in the leaving state, it outputs information on the passenger to the *outPerson* output port. If the cell is in the "returning" state, it outputs information on the returned passenger to the *outPerson* output port.

```
IF (Update=Ready)
  Output outCellInfo=Info
IF (Update=Updating)
  IF (Phase=Leaving)
    Output outPerson=Person
  IF (Phase=Returning)
    Output outPerson=inPerson
```

4.5. Internal transition function

If the cell is in the occupying or leaving state, its state will change to occupied or empty. If the cell is ready and occupied, it will update its own state based on the updating rules described in Section 3, and will check if the passenger in the current cell has left or not.

```
IF (Update=Ready)
  Update=Updating
IF (Phase=Occupied)
  UpdateCrowdBehavior (Neighbors)
  UpdateCounterflowAvoidingBehavior (Neighbors)
  Info=UpdateTotalScore ()
  IF (Info.IsMoving=True)
    Phase=Leaving
IF (Update=Updating)
  IF (Phase=Leaving)
    Phase=Empty, Person=Null
  IF (Phase=Returning or occupying)
    Phase=Occupied, Update=Ready
```

Table 1
Tests for the verification of the advanced evacuation analysis programs recommended by IMO MSC/Circ. 1238.

Test No.	Item
Test 1	Maintaining the set walking speed on a corridor
Test 2	Maintaining the set walking speed up a staircase
Test 3	Maintaining the set walking speed down a staircase
Test 4	Exit flow rate
Test 5	Response time
Test 6	Rounding corners
Test 7	Assignment of population demographic parameters
Test 8	Counterflow: Two rooms connected via a corridor
Test 9	Crowd dissipation from a large public room
Test 10	Exit route allocation
Test 11	Staircase

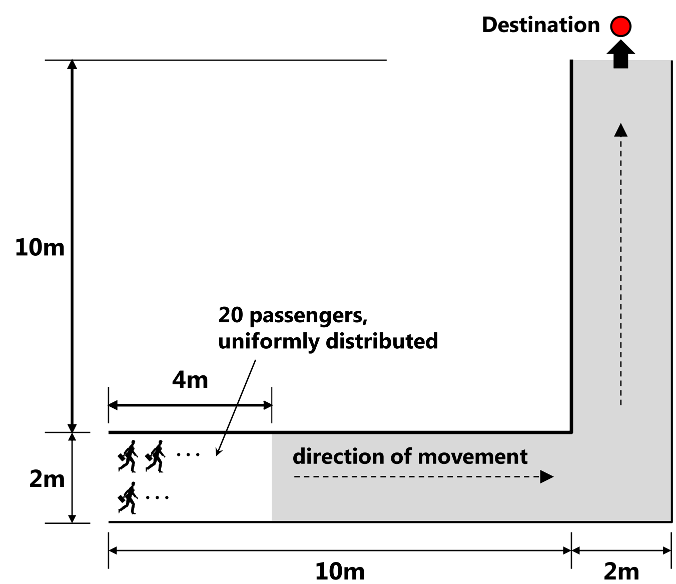

Fig. 13. Configuration of IMO test 6—rounding corners.

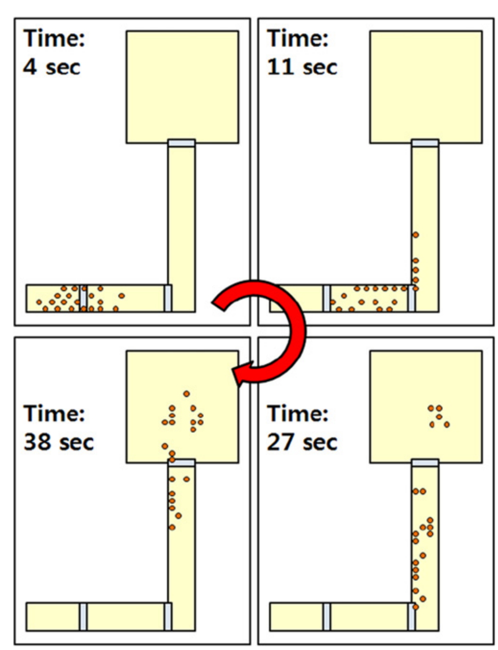

Fig. 14. Simulation results of IMO test 6—rounding corners.

4.6. Time advance

All the cells have the same intervals. If the current cell is ready, the cell will be triggered after an interval. If the current cell is in the updating state, it will change its phase directly. Otherwise, it will wait for the signal.

IF (***Update***=Ready)
  Wait for the *time step*
IF (***Update***=Updating)
  Wait for 0.0 s
OTHERWISE
  Wait for the ***signal***.

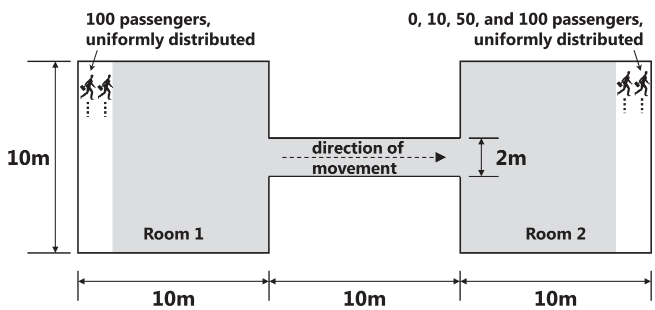

Fig. 15. Configuration of IMO test 8—counterflow, two rooms connected via a corridor.

5. Simulation and results

To verify the passenger behavior model proposed in this study, the 11 tests recommended by IMO/MSC Circ. 1238 ANNEX 3, and the examples of the compartments of the ship in IMO/MSC Circ. 1238 ANNEX 1, APPENDIX 2, were implemented. An application for carrying out an advanced evacuation analysis of a RORO passenger ship that can accommodate 1892 passengers was also performed to verify the program.

5.1. Verification of the passenger behavior model through IMO tests

To verify the proposed model, the 11 tests noted in the IMO/MSC Circ. 1238 Annex 3 guidance on the validation/verification of evacuation simulation tools were implemented. The tests included a check on whether the various components of the software were performing as intended. This test involved running the software through elementary test scenarios to ensure that the major subcomponents of the model were functioning as intended. Moreover, the tests concerned the nature of the predicted passenger behavior with informed expectations. The 11 tests recommended by IMO are listed in Table 1.

The results of the 11 tests verified the validity of the proposed model. In this paper, the detailed results of tests 6, 8, and 10 are described, as follows:

5.1.1. IMO test 6: rounding corners

Fig. 13 shows the configuration of IMO test 6, and Fig. 14 shows its simulation results. As shown in Figs. 13 and 20, passengers who

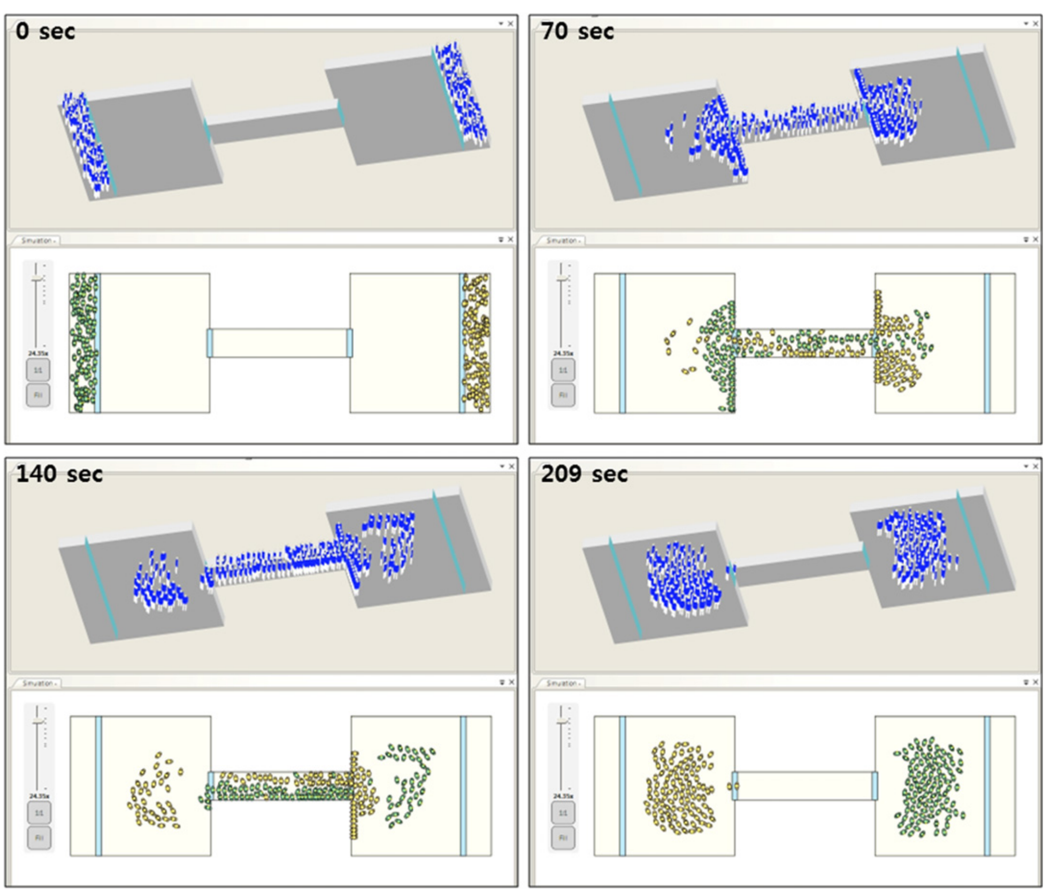

Fig. 16. Simulation results of IMO test 8–100 passengers in room 1 and 100 passengers in room 2.

were approaching a lefthand corner had to successfully navigate around the corner without penetrating the boundaries. All the passengers navigated around the corner without penetrating the wall, as shown in Fig. 14. They all stayed within the boundaries of the corridor or within the compartment's margins.

5.1.2. IMO test 8: Counterflow, two rooms connected via a corridor

Fig. 15 shows the configuration of IMO test 8, and Fig. 16 shows its simulation results. As shown in Fig. 15, two rooms, each 10-m wide and long, were connected via a corridor 10 m long and 2 m wide, starting and ending at the center of one side of each room. It was supposed that the passengers were 30- to 50-year-old males on a flat terrain, as mentioned in the appendix to the IMO Guidelines, and that their walking speeds were distributed over a population of 100 persons. For the first step of this test, 100 passengers moved from room 1 to room 2, wherein the initial distribution was such that the space of room 1 was filled from the left with the maximum possible density. Then step 1 was repeated with an additional 10, 50, and 100 passengers in room 2. These passengers had to have characteristics that were identical to those in room 1. Both rooms were simultaneously moved, and the time in which the last passenger in room 1 entered room 2 was recorded. The expected result was that the recorded time would increase with the number of passengers.

Table 2
Comparison of the total evacuation time in this study and that in Evi for IMO test 8 in IMO/MSC Circ. 1238.

No. of counterflow passengers	This study	Evi
0	84.6	88.9
10	93.2	125.6
50	137.1	229.1
100	216.1	327.9

It was confirmed that the total evacuation time increased relative to the increase in the number of passengers in room 2. Table 2 also shows that the total evacuation time in this study is less than that in Evi, a commercial program for advanced evacuation (Vassalos et al., 2002). This is assumed to be due to the different counterflow-avoiding algorithms applied in the programs.

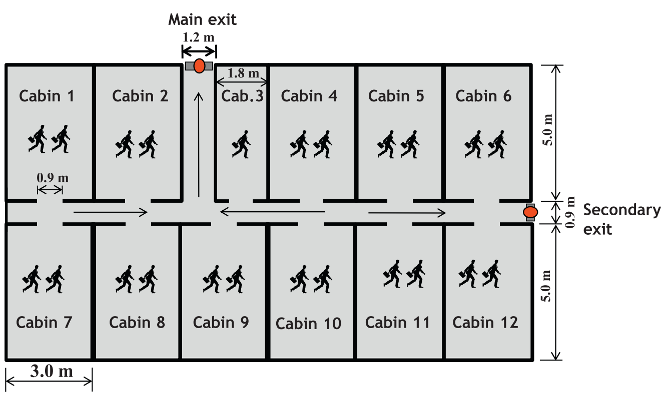

Fig. 17. Configuration of IMO test 11—exit route allocation.

5.1.3. IMO test 10: exit route allocation

Fig. 17 shows the configuration of IMO test 10, and Fig. 18 shows its simulation results. As shown in Fig. 17, a cabin corridor section was constructed, and 23 persons were distributed to each cabin. The people in cabins 1, 2, 3, 4, 7, 8, 9, and 10 were assigned to the main exit. All the remaining passengers were assigned to the secondary exit. The expected result is that the passengers move to their assigned exits. As shown in Fig. 18, the simulation results show that the people in cabins 1, 2, 3, 4, 7, 8, 9, and 10 indeed escaped through the main exit, and that the people in the other cabins indeed escaped through the secondary exit.

5.2. Comparison of the calculation time

For the calculation efficiency, this paper proposed a cell-based model. The calculation times were compared with those in the

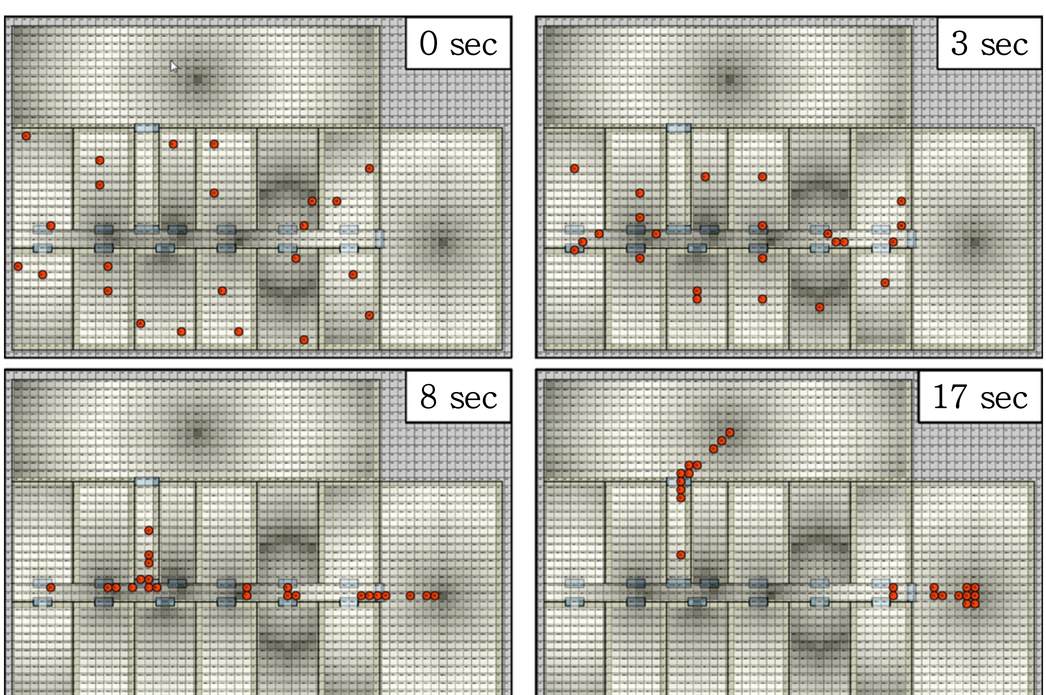

Fig. 18. Simulation results of IMO test 10—exit route allocation.

previous work by Cho (2011). Table 3 shows the calculation time for IMO test cases 8 and 9 of each research. It can also be seen that the proposed model is about two times more efficient than that in the previous work.

5.3. *Advanced evacuation analysis for RORO passenger ships*

In this section, the results of an advanced evacuation analysis that was conducted for a RORO passenger ship are presented. The simulation results are compared with the results of Evi.

There were nine decks and two assembly stations on deck 3, two assembly stations on deck 5, and four assembly stations on deck 7. The initial distribution corresponded to a total of 1892 persons located in the crew and passenger cabins. The initial distribution of the passengers is shown in Fig. 19.

The numbers of passengers at the assembly stations by time are plotted in Fig. 20. As the travel time was simulated as 14 min and 16 s, the total evacuation time was determined to be 37 min and 50 s. Therefore, it was confirmed that the requirement for total evacuation by IMO was satisfied in this RORO passenger ship. The difference in the travel time with Evi is 4.1, which can be considered almost inconsequential.

Table 3
Comparison of the calculation time with the previous work of Cho (2011).

Test case	Calculation time for each step (time step: 0.1 s)	
	Previous work (Cho, 2011)	**This paper**
Test Case #8 (No. of passengers: 1000)	0.530 s	0.231 s
Test Case #9 (No. of passengers: 200)	0.045 s	0.031 s

6. Conclusion

In this study, an advanced evacuation analysis that considers human behavior in a passenger ship was performed. Passenger behavior consists of individual, crowd, and counterflow-avoiding behaviors. Passenger behavior, which was proposed by Cho, was modeled using Cell-DEV and was verified with the 11 tests specified in IMO MSC/Circ. 1238. Advanced evacuation analysis was performed for a RORO passenger ship that could accommodate 1892 passengers. It was confirmed that the total evacuation time met the requirements. The simulation result was compared with that obtained with the commercial program for advanced evacuation analysis Evi, and it was confirmed that they differed by only 5%.

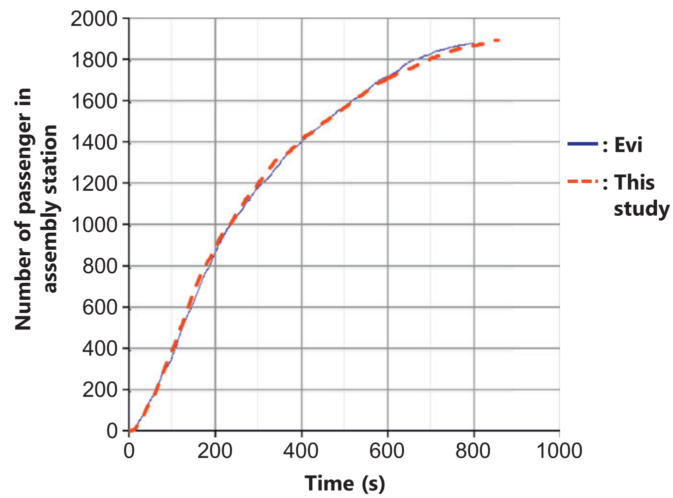

Fig. 20. Comparison of the results of the simulation with Evi: Number of passengers at the assembly stations.

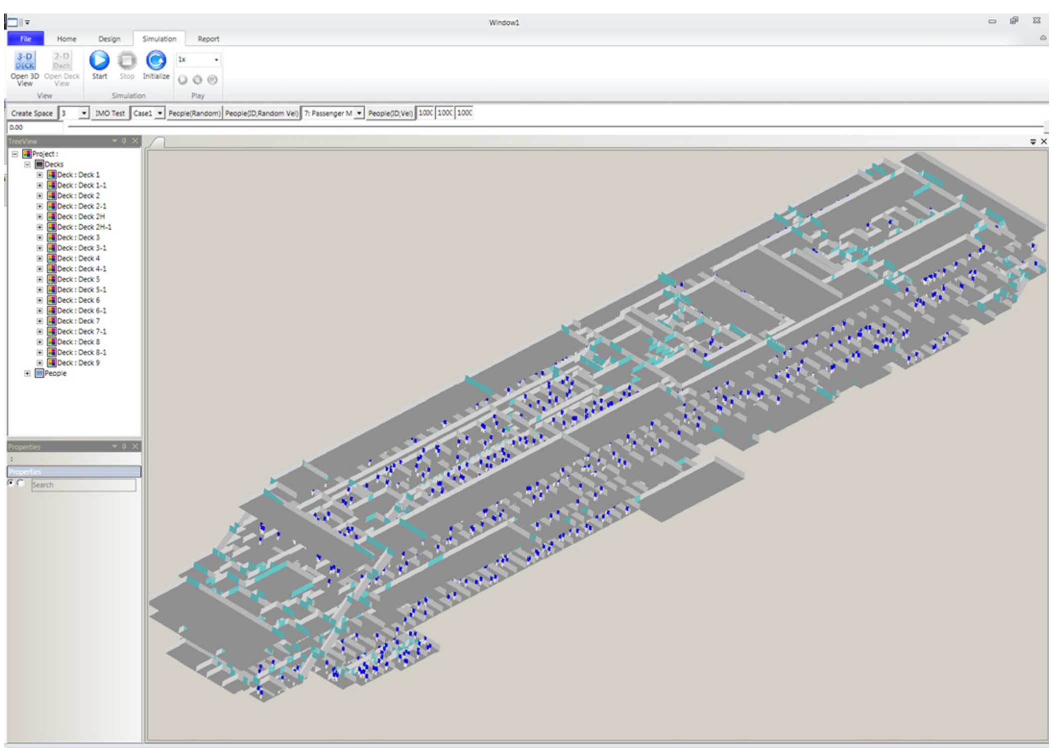

Fig. 19. Example of a RORO passenger ship: 3D view.

Acknowledgement

This work was partially supported by:

(a) Daewoo Shipbuilding & Marine Engineering Co., Ltd.;
(b) "SM-11: A Study on the Network-based Architecture of the Virtual System for the Simulation of Underwater Vehicles" of the Underwater Vehicle Research Center;
(c) Industrial Strategic Technology Development Program (10035331, Simulation-based Manufacturing Technology for Ships and Offshore Plants) funded by the Ministry of Knowledge Economy, South Korea;
(d) BrainKorea 21 by the Marine Technology Education and Research Center of Seoul National University;
(e) Research Institute of Marine System Engineering of Seoul National University; and
(f) New & Renewable Energy of the Korea Institute of Energy Technology Evaluation and Planning (KETEP) grant funded by the Korea Government Ministry of Knowledge Economy (No. 20114030200050).

References

Bang, K.W., 2006. Combined Discrete Event and Discrete Time Simulation Framework for Shipbuilding Process Planning. Master Thesis. Seoul National University, Seoul, Korea.

Cha, J.H., Lee, K.Y., Ham, S.H., Roh, M.I., Park, K.P., Suh, H.W., 2009. Discrete event/discrete timesimulation of block erection by a floating crane based on multibody system dynamics. In: 19th International Offshore and Polar Engineering Conference (ISOPE), Osaka International Convention Center, Osaka, Japan, vol. 3, pp. 678–685.

Cha, J.H., Roh, M.I., Lee, K.Y., 2010. Combined discrete event and discrete time simulation framework and its application to the block erection process in shipbuilding. Adv. Eng. Softw. 41 (4), 656–665.

Cho, Y.O., 2011. Advanced Evacuation Analysis considering Passenger Behavior in an Emergency. Master Thesis. *Seoul National University*, Seoul, Korea.

Cho, Y.O., Cha, J.H., Park, K.P., Ku, N.K., Ham, S.H., Lee, C.Y., Lee, K.Y., 2010. Determination of optimal walking direction for passenger evacuation using walking direction potential function and implementation of evacuation simulation. In: Proceedings of the Society of Naval Architecture of Korea 2010, Changwon, Korea, pp. 163–171. 11.

Ha, S., Cha, J.H., Lee, K.Y., 2009. HLA interface for combined discrete event & discrete time simulation model in distributed environment. In: Asia Simulation Conference, 2009, Ritsumeikan University, Shiga, Japan, October 7–9.

Ha, S., Cha, J.H., Park, K.P., Cho, Y.O., Lee, J.C., Lee, K.Y., 2011. Cell-based discrete event and discrete time simulation form the prediction of oil slick movement and spreading in ocean environment. In: Proceeding of the Society of CAD/CAM Engineers in Korea 2011, Pyongchang, Korea, pp. 544–551.

Hartman, C., Benes, B., 2006. Autonomous boids. Comput. Anim. Virtual Worlds 17, 199.

Helbing, D., Farkas, I., Vicsek, T., 2000. Simulating dynamical features of escape panic. Nature 407, 487–490.

Helbing, D., Molnar, P., 1995. Social force model for pedestrian dynamics. Phys. Rev. E 51 (5), 4282–4286.

IMO, 2007. Guidelines for evacuation analysis for new and existing passenger ships, IMO MSC/Circ.1238.

Kirchner, A., Klupfel, H., Nishinari, K., Schadschneider, A., Schreckenberg, M., 2003. Simulation of competitive egress behavior: comparison with aircraft evacuation data. Physica A 324, 689–697.

Kirchner, A., Schadschneider, A., 2002. Simulation of evacuation processes using a bionics-inspired cellular automaton model for pedestrian dynamics. Physica A 312, 260–276.

Praehofer, H., 1992. System theoretic foundations for combined discrete-continuous system simulation. VWGO.

Reynolds, C., 1987. Flocks, herds and schools: a distributed behavioral model. Comput. Graph. (ACM) 21 (4), 25–34.

Reynolds, C., 1999. Steering behaviors for autonomous characters. In: 1999 Game Developers Conference, San Jose, California, pp. 763–782.

Seyfried, A., Steffen, B., Lippert, T., 2006. Basics of modeling the pedestrian flow. Physica A 368, 232–238.

Song, W.G., Yu, Y.F., Wang, B.H., Fan, W.C., 2006. Evacuation behavior at exit in CA model with force essentials: a comparison with social force model. Physica A 371, 658–666.

Vassalos, D., Kim, H., Christiansen, G., Majumder, J., 2002. A Mesoscopic model for Passenger Evacuation in a Virtual Ship-Sea Environment and Performance-Based Evaluation, Pedestrian and Evacuation Dynamic. Springer, Netherlands, pp. 369–391.

Von Neumann, J., 1966. Theory of Self-reproducing Cellular Automata. University of Illinois Press, Urbana.

Wainer, G.A., Giambiasi, N., 2002. N-dimensional Cell-DEVS. Discrete Events Syst. Theory Appl. 12, 135–157.

Wainer, G.A., 2009. Discrete-Event Modeling and Simulation: A Practitioner's Approach. CRC.

Weng, W.G., Chen, T., Yuan, H.Y., Fan, W.C., 2006. Cellular automaton simulation of pedestrian counter flow with different walk velocities. Phys. Rev. E 74, 036102.

Yu, Y.F., Song, W.G., 2007. Cellular automaton simulation of pedestrian counter flow considering the surrounding environment. Phys. Rev. E 75, 046112.

Zeigler, B.P., Praehofer, H., Kim, T.G., 2000. Theory of modeling and simulation. Academic press, New York.

Zhao, D.L., Yang, L.Z., Li, J., 2006. Exit dynamics of occupant evacuation in an emergency. Physica A 363, 501–511.

Zheng M.H., Kushimori, Y., Kumbura, T., 2002. A model describing collective behaviors of pedestrians with various personalities in danger situations. In: Proceedings of the 9th international conference on neural information processing (ICONIP'02), vol. 4, pp. 2083–2087.